ELSEVIER

International Journal of Solids and Structures 41 (2004) 4875–4888

INTERNATIONAL JOURNAL OF SOLIDS and STRUCTURES

www.elsevier.com/locate/ijsolstr

A comprehensive stability analysis of a cracked beam subjected to follower compression

Q. Wang *

Mechanical, Materials and Aerospace Engineering Department, University of Central Florida, P.O. Box 162450, 4000 Central Florida Blvd., Orlando, FL 32816-2450, USA

Received 20 April 2004; received in revised form 20 April 2004
Available online 25 May 2004

Abstract

A comprehensive analysis of the stability of a cracked beam subjected to a follower compressive load is presented. The beam is fixed at its left end and restrained by a translational spring at its right end. The vibration analysis on such cracked beam is conducted to identify the critical compression load for flutter or buckling instability based on the variation of the fist two resonant frequencies of the beam. Besides, the effect of the crack's intensity and location on the buckling or flutter compressive load is studied through comprehensive mechanics analysis. It is hoped that this research may provide a benchmark on the stability analysis of cracked structures in engineering applications, especially for structures subjected to follower compressive load.

Keywords: Stability of structures; Buckling; Flutter; Follower force; Non-follower force; Vibration analysis

1. Introduction

Analysis of flutter and buckling of beams has attracted attention in the applied mechanics community for long. The mathematical solutions for the buckling load of beams subjected to non-follower compression with different boundary conditions were given in the monograph by Timoshenko and Gere (1961). In addition, flutter analysis of a cantilever beam subjected to follower compression was also briefly introduced in the monograph. Beam buckling is an instability phenomenon where change of equilibrium state from one configuration to another occurs at a critical compression value. On the other hand, flutter is an instability phenomenon where the vibration amplitude due to initial disturbance grows without limit when the follower compression exceeds a critical value.

Buckling and flutter analysis of healthy or undamaged beam structures under follower force has been improved by many research efforts. Bolotin (1963) studied a classical problem about the stability of a beam fully fixed at one end and subjected at the other end to a tangential compressive follower force. Feodosév

* Corresponding author. Tel.: +1-407-8235828; fax: +1-407-8230208.
E-mail address: qzwang@mail.ucf.edu (Q. Wang).

0020-7683/$ - see front matter © 2004 Published by Elsevier Ltd.
doi:10.1016/j.ijsolstr.2004.04.037

(1953) and Pfluger (1950) showed that there are no buckling solutions for this problem and concluded that the beam with follower force is stable all the time. This erroneous conclusion was debated by Beck (1952) who first solved this flutter instability problem through dynamic analysis. Since then the study of flutter instability has attracted substantial research interest. The critical follower force for the flutter of a cantilever beam was evaluated by Deineko and Leonov (1955). A more accurate critical load was obtained by Jankovic (1993). Carr and Malhardeen (1979) and Leipholz (1983) proved that Beck's column is stable when the follower force is less than the critical value obtained by Beck. Dzhanelidze (1958) studied the combined effect of non-follower and follower compressions applied to a cantilever beam. Hauger and Vetter (1976) studied the influence of elastic foundation of Winkler type on the stability of Beck's column. The influence of pulsating force was investigated by Atanackvic and Cveticanin (1994). The optimal shape of Beck's column was given by Hanaoka and Washizu (1979). Matsuda et al. (1993) studied the effects of variable cross-section and shear stresses on the value of the critical force. The influence of an elastic support on the vibration and stability of a non-conservative load was studied by Sundararajan (1976). In his paper, the transition value of the translational spring at the free end of a cantilever beam was derived, and the co-existence of flutter and buckling in a system was first observed. Kounadis (1983) presented an analysis of the existence of divergence instability regions for a general beam structure. Sugiyama and his group (1995) and his group did a lot of excellent work on the flutter analysis of structures. One experimental study was on the flutter of cantilevered columns under rocked thrust, which was one of the best lab demonstrations of follower compression on beam structures. Wang and Quek (2002) investigated the potential of applying piezoelectric materials in the enhancement of the flutter and buckling load of the beam structures.

More research on the buckling and/or flutter load of cracked beams subjected to follower compression is critical for a better design and health monitoring of such beams. Cracks occurring in structural elements, such as beams and plates, affect the dynamic characteristics of structures. The understanding of the cracks' effect is essential in the design of structures and important in the damage detection of structures. For example, the study of the crack effects on the reductions of frequencies has led to the identification and detection of cracks (Cawley and Adams, 1979). In addition, the understanding of the reduction in buckling and/or flutter load due to cracks is also of great importance in the repair design of structures in civil, mechanical and aerospace engineering. The models for cracked beams have been proposed and applied to various engineering problems by many researchers so far. The stability of a cracked column was studied experimentally and analytically (Liebowitz et al., 1967; Anyfantis and Dimarogonas, 1983; Dimarogonas and Paipetis, 1983) by considering the local flexibility by the crack as a spring. Dimarogonas and Paipetis (1983) developed a general method to identify all the possible direct and coupling spring effects for a prismatic beam with a surface crack. Paradopoulos and his students have investigated the coupling effect of cracks on structures (Kikidis and Papadopoulos, 1992; Papadopoulos, 1994; Gounaris et al., 1996; Nikolakopoulos et al., 1967; Gounaris and Papadopoulos, 1997). They used local flexibility method to model cracks and derived the flexibility matrix based on linear elastic fracture mechanics. However, few reports have been found on the analyses of the buckling and/or flutter load of cracked beams subjected to follower compression.

This paper will provide a comprehensive instability analysis of a cracked beam subjected to a follower compressive load. This beam is fixed at the left end and restrained by a translational spring at its right end. Preliminary research on the critical spring stiffness under which flutter may occur and above which buckling may occur has been identified by Wang and Koh (2003). In the current research, the flutter or buckling load of a cracked beam will be obtained through dynamic analysis of the beam. The effect of the crack's intensity and location on the buckling or flutter load will be provided via a detailed mechanics analysis. The research method is strictly based on an undamped linearized approach. The co-existing instability phenomena of the cracked beam structure is interesting in the field of structural stability and dynamics, as the understanding of the instability nature of a cracked beam structure will be helpful for its stability design. Therefore, the research results will be useful for the design and control of damaged structures.

2. Mechanics model for the stability analysis

A cracked beam structure under a follower force P at its right end is shown in Fig. 1. This beam is fixed at the left end and restrained by a translational spring with stiffness k at the right end. The beam of thickness h and length L is isotropic with Young's modulus E, mass density ρ and cross-area A. A vertical surface crack, with depth h_1, is located at a distance L_1 from the left end of the beam. Let x be the coordinate denoting the beam length with its origin at the left end, and u the beam deflection defined to be positive downward. As the ratio, L/h, in buckling problems is usually large, the effects of shear deformation and rotary inertia may be neglected.

The presence of a crack in the mechanics model can be represented by a discontinuity in the slope at the location of the crack (Krawczuk and Ostachowicz, 1995). The total change of the slope of the beam at $x = L_1$, the continuity of the deflection, rotation, and the shear at the crack location are modeled as

$$\left.\frac{\mathrm{d}u_2}{\mathrm{d}x}\right|_{x=L_1} - \left.\frac{\mathrm{d}u_1}{\mathrm{d}x}\right|_{x=L_1} = \Theta \left.\frac{\mathrm{d}^2u_1}{\mathrm{d}x^2}\right|_{x=L_1} \tag{1}$$

$$u_1(L_1) = u_2(L_1); \quad \left.\frac{\mathrm{d}^2u_1(x)}{\mathrm{d}x^2}\right|_{x=L_1} = \left.\frac{\mathrm{d}^2u_2(x)}{\mathrm{d}x^2}\right|_{x=L_1}; \quad \left.\frac{\mathrm{d}^3u_1(x)}{\mathrm{d}x^3}\right|_{x=L_1} = \left.\frac{\mathrm{d}^3u_2(x)}{\mathrm{d}x^3}\right|_{x=L_1} \tag{2a–c}$$

where $u_1(x)$ and $u_2(x)$ represent the deflection field of the beam for the domains of $0 < x < L_1$ and $L_1 \leqslant x < L$, respectively. The parameter Θ represents the additional flexibility of the beam due to the crack calculated on the basis of fracture mechanics and Castigliano theorem shown below:

$$\Theta = 6\pi H \int_0^{\bar{a}} [\bar{a} F_{15}^2(\bar{a})]\,\mathrm{d}\bar{a} \tag{3}$$

where $\bar{a} = h/H$. $F_{15}(\bar{a})$ is a correction function for stress intensity factor corresponding to a beam structure, given by

$$F_{15}^2(\bar{a}) = \sqrt{\tan(\pi\bar{a}/2)/(\pi\bar{a}/2)}[0.923 + 0.199(1 - \sin(\pi\bar{a}/2))^4]/\cos(\pi\bar{a}/2).$$

The above-proposed model for the discontinuity of the rotation at the crack location in Eq. (1) is only valid for a composite beam with a transverse open crack (Krawczuk and Ostachowicz, 1995).

The stability analysis of the beam structure will be obtained from a free vibration analysis conducted hereinafter. The governing equation of the cracked beam under the follower force P in Fig. 1 is given by the following equation,

$$\mathrm{EI}\frac{\partial^4 u(x,t)}{\partial x^4} + P\frac{\partial^2 u(x,t)}{\partial x^2} + \rho A\frac{\partial^2 u(x,t)}{\partial t^2} = 0. \tag{4}$$

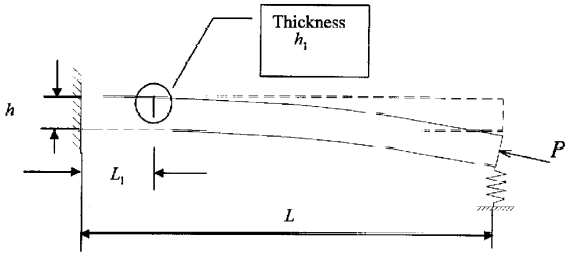

Fig. 1. A cracked beam fixed at left end and elastically restrained at right end subjected to a follower force.

By using variable separation method, $u(x,t) = U(x)e^{i\omega t}$, we may find the analytical solution for the function $U(x)$ directly as follows,

$$U_1(x) = A_1\cos k_1x + A_2\sin k_1x + A_3\cosh k_2x + A_4\sinh k_2x \quad 0 < x < L_1 \tag{5}$$

$$U_2(x) = B_1\cos k_1x + B_2\sin k_1x + B_3\cosh k_2x + B_4\sinh k_2x \quad L_1 \leqslant x < L \tag{6}$$

where $k_1 = \left(\frac{\lambda}{2} + \sqrt{\frac{\lambda^2}{4} + \mu^2}\right)^{1/2}$; $k_2 = \left(-\frac{\lambda}{2} + \sqrt{\frac{\lambda^2}{4} + \mu^2}\right)^{1/2}$; and $\lambda = \frac{P}{EI}$ and $\mu^2 = \frac{\rho A\omega^2}{EI}$.

The boundary conditions of the cracked beam are shown below

$$U_1(0) = 0, \quad \left.\frac{dU_1(x)}{dx}\right|_{x=0} = 0 \tag{7a–b}$$

$$\left.\frac{d^2U_2(x)}{dx^2}\right|_{x=L} = 0, \quad \left.\frac{d^3U_2(x)}{dx^3}\right|_{x=L} - \frac{\bar{k}}{L^3}U_2(L) = 0 \tag{8a–b}$$

where the non-dimensional spring stiffness is given by $\bar{k} = \frac{kL^3}{EI}$.

Substituting the boundary conditions in Eq. (7a–b) into Eq. (5) yields

$$U_1(x) = A_3(\cosh k_2x - \cos k_1x) + A_4\left(\sinh k_2x - \frac{k_2}{k_1}\sin k_1x\right) \tag{9}$$

Similarly, $U_2(x)$ may be expressed in terms of B_3 and B_4 by substituting Eq. (8a–b) into Eq. (6) as follows

$$U_2(x) = B_3(\cosh k_2x + N_1\cos k_1x + N_3\sin k_1x) + B_4(\sinh k_2x + N_4\sin k_1x + N_2\cos k_1x) \tag{10}$$

where $N_i (i = 1,2,3,4)$ are given in the appendix.

The continuity conditions on the shear force and moment shown in Eq. (2b) and Eq. (2c)at the crack location lead to the following equations,

$$P_1A_3 + P_2A_4 + P_3B_3 + P_4B_4 = 0 \tag{11}$$

and

$$Q_1A_3 + Q_2A_4 + Q_3B_3 + Q_4B_4 = 0 \tag{12}$$

from which A_3 and A_4 can be expressed in terms of B_3 and B_4 as follows,

$$A_3 = R_1B_3 + R_2B_4 \tag{13a}$$

$$A_4 = R_3B_3 + R_4B_4 \tag{13b}$$

P_i, Q_i and R_i $(i = 1,2,3,4)$ are shown in appendix.

Substituting Eqs. (5) and (6) into continuity on the deflection in Eq. (2a) and the discontinuity condition on the slope in Eq. (1) while considering the expressions of A_3 and A_4 in terms of B_3 and B_4 shown in Eqs. (13a) and (13b) yields

$$\Delta_1B_3 + \Delta_2B_4 = 0 \tag{14}$$

$$\Delta_3B_3 + \Delta_4B_4 = 0 \tag{15}$$

where $\Delta_i (i = 1,2,3,4)$ are given in appendix.

The instability of the beam, either for buckling or flutter, will be derived from the condition for the non-trivial solution for B_3 and B_4 from Eqs. (14) and (15), which is,

$$\Delta_1\Delta_4 - \Delta_2\Delta_3 = 0 \tag{16}$$

The procedure for obtaining the flutter or buckling load of the cracked beam subjected to the follower force will be provided below. For a given follower force P, the first two resonant frequencies ω_1 and ω_2 can be obtained from Eq. (16). There is, however, a definite value of the follower force P at which the values of ω_1 and ω_2 approach each other (Timoshenko and Gere, 1961). We define the definite value of the follower force as the flutter load of the beam structure. On the other hand, we define the value of the follower force as the buckling load of the structure where the value of ω_1 reaches zero.

3. Numerical results and discussion

Numerical simulations are conducted for a comprehensive stability analysis of the cracked beam structure under follower force in Fig. 1. The length of the beam is $L = 1$ m and the depth of the beam is $h = 0.05$ m. The following non-dimensional parameters will be employed in the simulations: frequency of the beam $\varpi = \omega L^2\sqrt{\frac{\rho A}{EI}}$; follower force $\bar{P} = P/P_{cr}$ where $P_{cr} = \pi^2 EI/L_2$ is Euler buckling load; the location of crack $\bar{L}_1 = L_1/L$, the coordinate in the length direction of the beam $\bar{x} = x/L$, and the spring stiffness given $\bar{k} = \frac{kL^3}{EI}$.

First, the critical load for a healthy beam versus the stiffness of the spring at the right end of the beam is plotted in Fig. 2 for comparison. An abrupt decrease of the load at $\bar{k} \approx 34.8$ is clearly observed from the figure. From the variation of the first two frequency of the system, it can be concluded that $\bar{k} \approx 34.8$ is the critical stiffness of the spring differentiating flutter and buckling instability of the beam. If the stiffness of the spring is less than the critical value, only flutter may occur on the beam under follower compression, otherwise, only buckling instability will occur on the beam. This conclusion was also cited by Kounadis (1983). The critical compressive load for flutter of a cantilever beam and for buckling of a propped cantilever beam can be read from Fig. 2 as $\bar{P} = 2.04$ and $\bar{P} = 2.05$ if $\bar{k} = 0$ and $\bar{k} = \infty$ are set. These results are in agreement with those from the monograph of Timoshenko and Gere (1961). The value of the spring stiffness differentiating the buckling and flutter in the beam structure is defined as transition value of the stiffness. For example, $\bar{k}_{ch} \approx 34.8$ is the transition value of the spring stiffness for a healthy beam.

Next, we use $\bar{k}_c$ as the critical value of the spring stiffness in the cracked beam. The solution for $\bar{k}_c$ versus the crack location is plotted in Fig. 3 at different values of additional flexibility, $\Theta = 0$, $\Theta = 0.05$, and $\Theta = 0.1$ (Wang and Koh, 2003). These values of the additional flexibility represent the ratios of the crack's

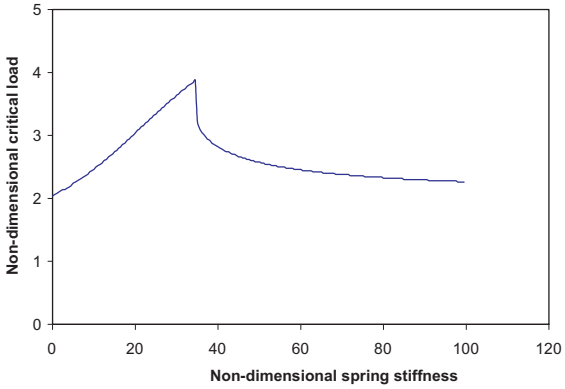

Fig. 2. Critical compressive load versus the non-dimensional spring stiffness.

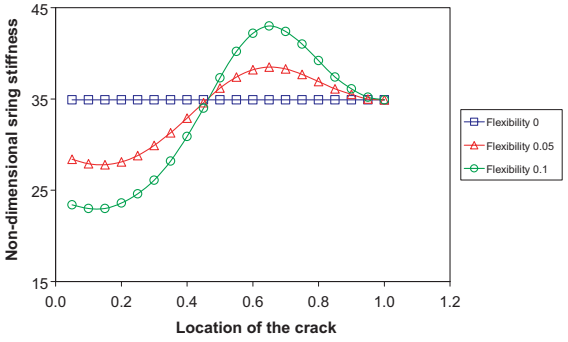

Fig. 3. Critical spring stiffness versus crack location.

depth to the beam's depth as $\frac{h_1}{h} = 0$, 0.40, and 0.50 respectively from the conclusion based on Eq. (3). It is observed that $\bar{k}_c$ is smaller compared to that of the healthy beam, i.e. $\bar{k}_{ch} = 34.85$, when the crack is located at $\bar{L}_1 < 0.45$. On the other hand, when the crack is located at $\bar{L}_1 \geqslant 0.45$, $\bar{k}_c$ is always bigger than $\bar{k}_{ch} = 34.85$. In addition, critical stiffness $\bar{k}_c$ converges to $\bar{k}_{ch}$ at $\bar{L}_1 = 1$, since it is understandable that the effect of the crack is negligible if it is located at the end with the translational spring. Another investigation is that the higher the intensity of the crack is (i.e. bigger Θ), the larger the difference is found between $\bar{k}_c$ and $\bar{k}_{ch}$. Two critical locations of the crack, $\bar{L}_1 \approx 0.45$ and $\bar{L}_1 = 1$, are found at which $\bar{k}_c = \bar{k}_{ch}$. A brief analysis for the above observation was given by Wang and Koh (2003).

The variation of the critical compressive load $\bar{P}$ in the instability of the beam versus the locations of the crack at $\Theta = 0$, 0.05, 0.1 is given in Fig. 4 at $\bar{k} = 0$. As indicated in Fig. 3, only flutter may occur in this case. Therefore, the capacities derived in this figure are the capacities of the follower force for flutter of the damaged beam. It is reasonable to observe that $\bar{P} = 2.04$ at $\Theta = 0$, where there is no crack at all. The results are in agreement with Timoshenko and Gere (1961)'s findings about a cantilever beam. Further observations from Fig. 4 show that the capacities are less than $\bar{P} = 2.04$ when the crack is placed at $\bar{L}_1 < 0.1$, whereas the capacities are bigger than $\bar{P} = 2.04$ when the crack is placed at $\bar{L}_1 > 0.1$. Furthermore, the difference between the compression load for the cracked beam and for its healthy counterpart where $\bar{P} = 2.04$ is bigger if the crack is deeper in the beam as clearly indicated in Fig. 4. These observations can be explained through the analysis of the flutter mode shapes of the displacement and the curvature of the beam

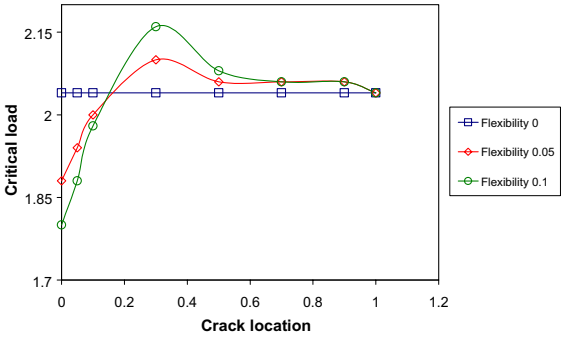

Fig. 4. Critical compressive load versus crack location at $\bar{k} = 0$.

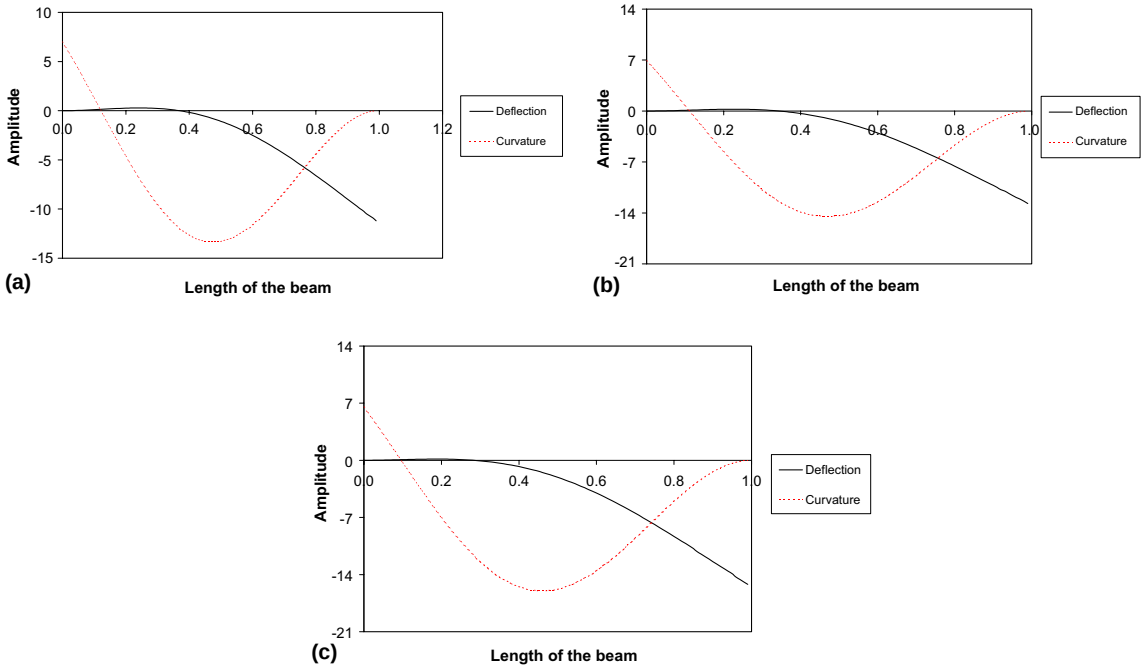

Fig. 5. (a) Mode shape at $\bar{k} = 0$ and $\Theta = 0$. (b) Mode shape at $\bar{k} = 0$ and $\Theta = 0.05$. (c) Mode shape at $\bar{k} = 0$ and $\Theta = 0.1$.

shown in Fig. 5 (a)–(c) for $\Theta = 0$, 0.05, and 0.1 separately. Since the location of the crack has little effect on the mode shape, the plots are provided at any crack location $\bar{L}_1$ for each case. It is observed from the variation of the mode shapes in Fig. 5(a)–(c) that the curvature of the cracked beam is positive to the left of position $\bar{x} \approx 0.1$ and becomes negative after this position and approach to zero where $\bar{x} = 1$. As explained before, the initiation of flutter instability is identified from the phenomenon that the first frequency of the cracked beam approaches to the second one. It is hence concluded from the mechanics model that the first mode shape of the displacement of the beam will change to its second mode shape at the initiation of the flutter. Thus, if the presence of the crack makes the beam prone to change its first mode shape to second one, the critical load $\bar{P}$ for flutter will decrease. Otherwise, $\bar{P}$ will increase. The analysis of the crack's effect on the critical load is hence conducted in Fig. 6. The mode shape of the displacement is as displayed in Fig. 5(a)–(c) with its right end bending downwards. In Fig. 6(a), the crack is located at $\bar{L}_1 > 0.1$ where the curvature is negative. According to Eq. (3), the slope at the right side of the crack will be smaller than the slope at the left side of the crack as shown in Fig. 6(a). In this case, the presence of the crack induces additional moment at the fixed end in Fig. 6(a) due to the follower force applied to the beam. The induced moment has the effect of making the beam bend further in its first mode shape but not towards the second mode shape. This effect will definitely increase the flutter load of the cracked beam. On the other hand, if the crack is located at $\bar{L} < 0.1$ where the curvature is positive in Fig. 6(b), the curvature at the crack location will be positive. Thus, the slope at the right side of the crack will be bigger than the slope at the left side of the crack. Therefore, the presence of the crack leads to additional induced moment as shown in Fig. 6(b) due to the follower force $\bar{P}$. This induced moment will make the beam change its vibration mode shape from the first mode shape to the second mode shape. The critical load will decrease hence after. The above investigations explain why the critical load $\bar{P}$ increases when the crack is located at $\bar{L}_1 > 0.1$, and decreases when the crack is located at $\bar{L}_1 < 0.1$ as shown in Fig. 4. The critical load for the cracked beam remains the

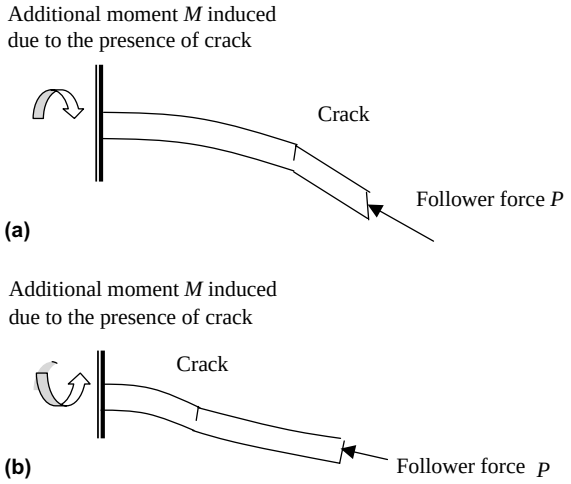

Fig. 6. (a) Crack effect on the mode transition; curvature at crack location is negative. (b) Crack effect on the mode transition; curvature at crack location is positive.

same as the critical load for a healthy beam if the crack is located at $\bar{L}_1 \approx 0.1$ and $\bar{L}_1 = 1$ since the curvature at these locations is zero and crack has no effect on the stability of the beam.

The critical load for the beam, the mode shapes of the displacement, and the curvature of the beam at $\bar{k} = 10$ are plotted in Figs. 7 and 8(a)–(c) respectively at $\Theta = 0$, 0.05, and 0.1. Fig. 3 shows that flutter is the only instability form for the beam. The critical load for the healthy beam can be read from Fig. 7 directly as $\bar{P} = 2.46$ when $\Theta = 0$. The curve shows that if the crack is located at $\bar{L}_1 < 0.05$ or $\bar{L}_1 > 0.75$, $\bar{P}$ for the occurrence of flutter is smaller than 2.46, $\bar{P}$ for the healthy beam. On the other hand, $\bar{P}$ is bigger than the value for the healthy beam if the crack is located in the region of $0.05 < \bar{L}_1 < 0.75$. These observations can be explained from the variation of the mode shape of curvature in Fig. 8(b)–(c) as well. The curves in these figures show that the curvature is positive when $\bar{x} < 0.05$ and becomes negative when $0.05 < \bar{x} < 0.75$. When $\bar{x} > 0.75$ the curvature becomes positive again. Thus, $\bar{L}_1 < 0.05$ nd $\bar{L}_1 > 0.75$ are two regions of the crack locations where the critical load will decrease as illustrated in Fig. 6(b).

The critical load $\bar{P}$, the corresponding mode shape of displacement, and curvature at $\bar{k} = 20$ are shown in Figs. 9 and 10(a)–(c) at $\Theta = 0$, 0.05, and 0.1 respectively. When the crack's location is in the two regions of where curvatures are positive, $\bar{P}$ is less than the value for healthy beam as explained before. The two regions

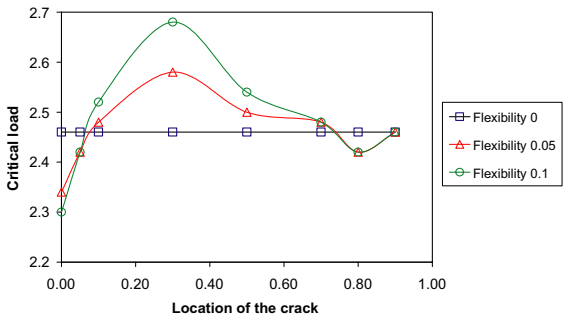

Fig. 7. Critical compressive load versus crack location at $\bar{k} = 10$.

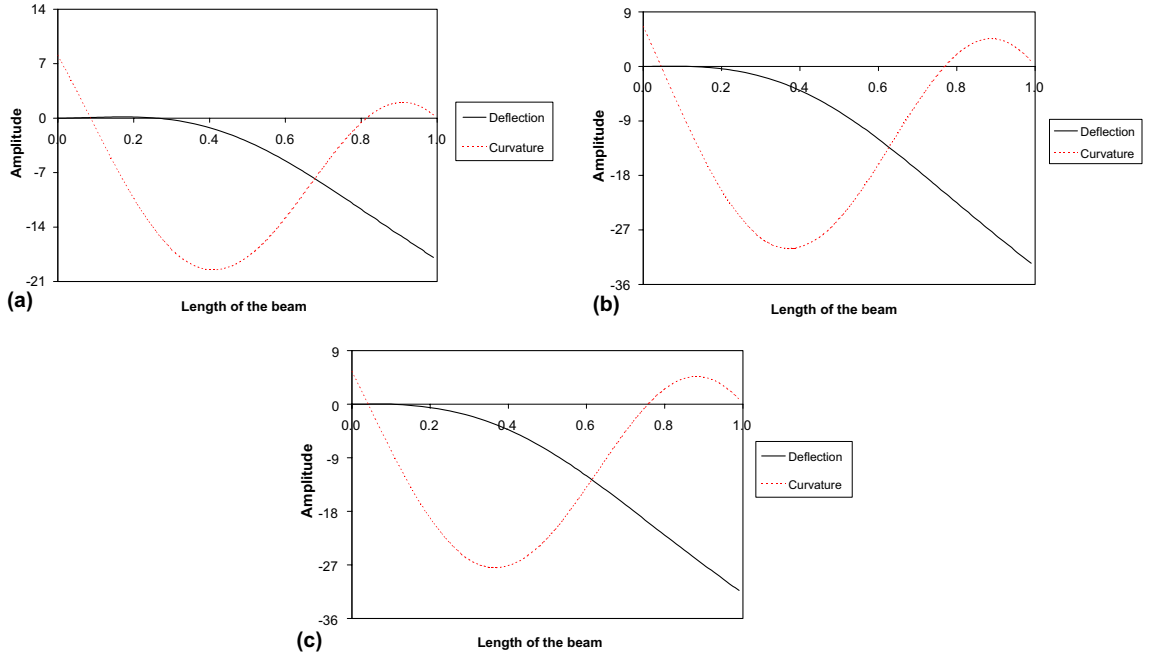

Fig. 8. (a) Mode shape at $\bar{k} = 10$ and $\Theta = 0$. (b) Mode shape at $\bar{k} = 10$ and $\Theta = 0.05$. (c) Mode shape at $\bar{k} = 10$ and $\Theta = 0.01$.

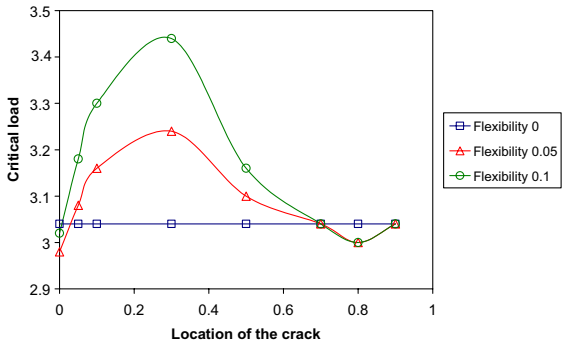

Fig. 9. Critical compressive load versus crack location at $\bar{k} = 20$.

move leftward with higher intensity of the crack in this simulation. For example, the two regions are $0 < \bar{x} < 0.03$ and $0.62 < \bar{x} < 1$ at $\Theta = 0.05$. But for a deeper crack, $\Theta = 0.1$, the first region disappears and the second region becomes $0.58 < \bar{x} < 1$. The critical load for a healthy beam is $\bar{P} = 3.4$ in this case.

The critical load $\bar{P}$ for $\bar{k} = 80$, the mode shapes for the displacement, and the curvature at $\Theta = 0$, 0.05, and 0.1 are plotted in Figs. 11 and 12(a)–(c) respectively. From the critical spring stiffness shown in Fig. 3, it is clear that the instability for the beam at $\bar{k} = 80$ is only the buckling form. The buckling load for a healthy beam is $\bar{P} = 2.32$ as shown in Fig. 11 at $\Theta = 0$. The mode shape for the curvature of the cracked beam for this case is negative in the region of $0 < \bar{x} \leqslant 0.35$ and becomes positive when $\bar{x} > 0.35$. Surprisingly, the buckling load for a cracked beam on the first region with negative curvature is less than the value for the

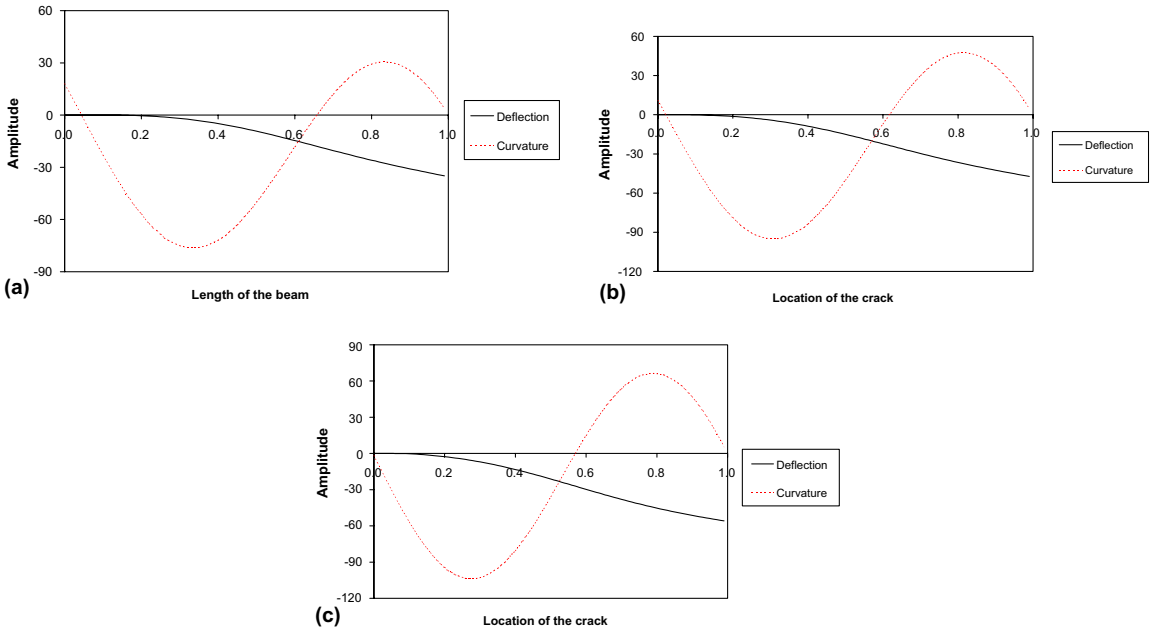

Fig. 10. (a) Mode shape at $\bar{k} = 20$ and $\Theta = 0$. (b) Mode shape at $\bar{k} = 20$ and $\Theta = 0.05$. (c) Mode shape at $\bar{k} = 20$ and $\Theta = 0.1$.

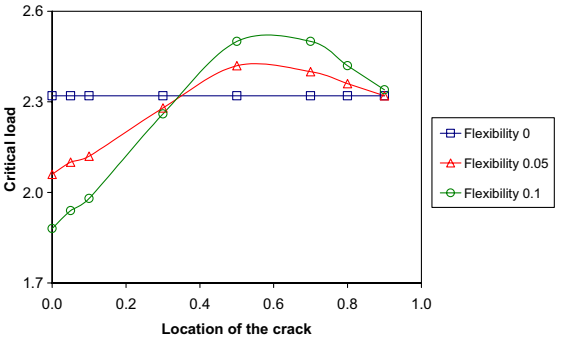

Fig. 11. Critical compressive load versus crack location at $\bar{k} = 80$.

healthy beam. This is completely opposite to what we obtained previously for the flutter load of the cracked beam. This phenomenon can also be explained from mode transition shown in Fig. 6. In Fig. 6(b), since the mode shape for the curvature is negative at $0 < \bar{x} < 0.35$, the induced additional moment due to a crack located in this region will make the vibration mode of the beam change from the first mode shape to its second mode shape. This tendency of mode transition will definitely increase the critical load because the first buckling load is always smaller than the second one. This analysis can also explain why the critical load becomes smaller when the crack is located in the region $0.35 < \bar{x} < 1$ where the curvature is positive. The buckling load of a cracked beam under non-follower compression will definitely always be smaller than its healthy counterpart. This is because no additional moment is induced due to the presence of the crack when there is no shear component from the non-follower force. The reason for the reduction of the buckling load

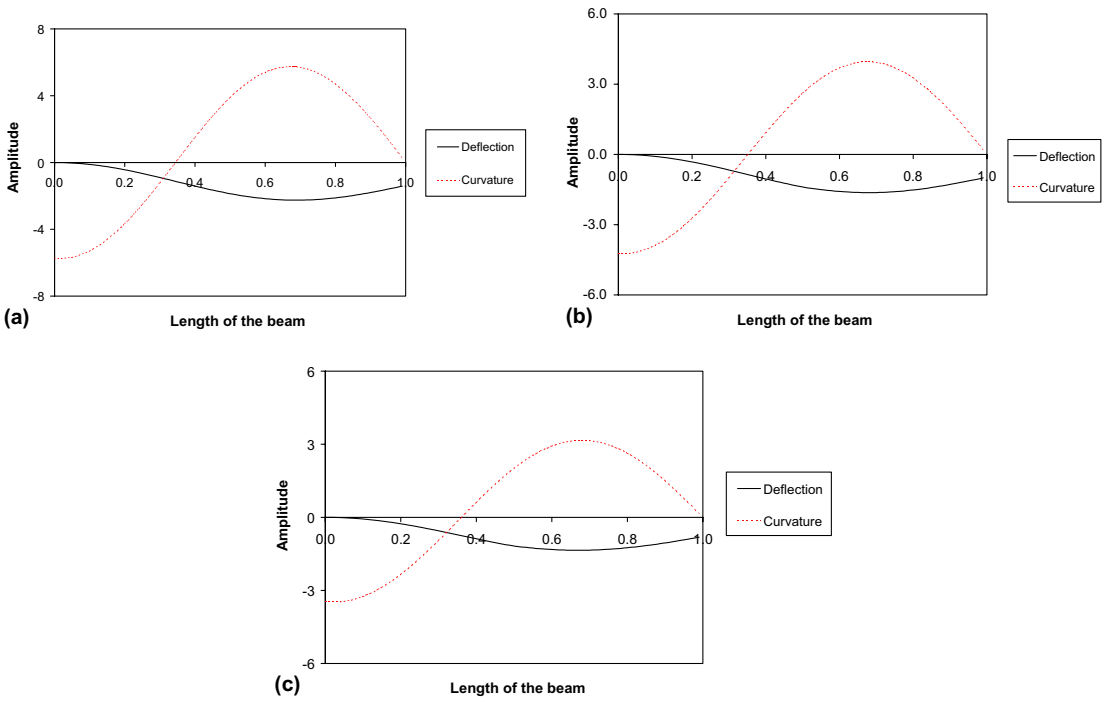

Fig. 12. (a) Mode shape at $\bar{k} = 80$ and $\Theta = 0$. (b) Mode shape at $\bar{k} = 80$ and $\Theta = 0.05$. (c) Mode shape at $\bar{k} = 80$ and $\Theta = 0.1$.

for a cracked beam under non-follower force is that the crack makes the stiffness of the beam decrease so that the beam buckles easier.

In Fig. 13, the critical load $\bar{P}$ is provided at $\bar{k} = 40$. The shape of the curve in the region of $0 < \bar{x} < 0.4$ is similar to that in Fig. 11 since the beam with crack at this region may only buckle as indicated in Fig. 3. However, when the crack is near $\bar{L}_1 = 0.7$, the instability of the beam will be flutter as indicated in Fig. 3. This is why the curve around $\bar{L}_1 = 0.7$ changes dramatically in a very short region due to the transition between buckling and flutter.

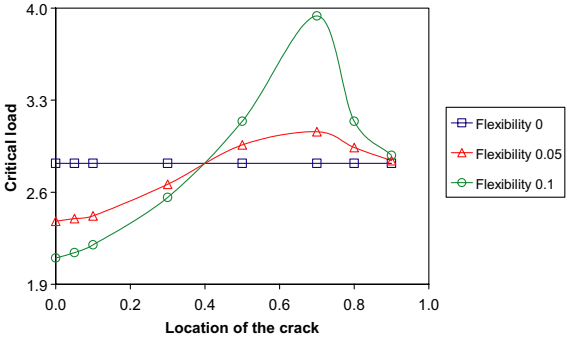

Fig. 13. Critical compressive load versus crack location at $\bar{k} = 40$.

4. Conclusions

This paper presents a comprehensive stability analysis of a cracked beam, with the left end fixed and the right end restrained by a translational spring, subjected to a follower compressive force. Extensive studies on the critical load for beam instability versus crack location have been conducted. The effect of the crack on the critical load can be explained from the distribution of the mode shape of the displacement and the curvature. These findings are based on the assumption that the displacement mode shape is displayed with the right tip pointing downward. For flutter instability, flutter load will decrease if the crack is located in the region with positive curvature and increase otherwise to a greater extent compared with that of a healthy beam. On the contrary, for buckling instability, the buckling load will increase if the crack is located in the region with positive curvature and decrease otherwise. It is hoped that this research will provide a benchmark for the stability analysis of cracked beams. Further studies will be focused on the stability analysis of damaged plates or shells. The effects of cracks on these structures under either non-follower or follower compression need to be investigated.

Appendix A

$$N_1 = \frac{L_2M_3 - L_3M_2}{L_1M_2 - L_2M_1}, \quad N_2 = \frac{L_2M_4 - L_4M_2}{L_1M_2 - L_2M_1}, \quad N_3 = \frac{L_1M_3 - L_3M_1}{L_2M_1 - L_1M_2}, \quad N_4 = \frac{L_1M_4 - L_4M_1}{L_2M_1 - L_1M_2};$$

$$L_1 = -k_1^2 \cos k_1L, \quad L_2 = -k_1^2 \sin k_1L, \quad L_3 = k_2^2 \cosh k_2L, \quad L_4 = k_2^2 \sinh k_2L;$$

$$M_1 = k_1^3 \sin k_1L - \frac{\bar{k}}{L^3} \cos k_1L, \quad M_2 = -k_1^3 \cos k_1L - \frac{\bar{k}}{L^3} \sin k_1L,$$

$$M_3 = k_2^3 \sinh k_2L - \frac{\bar{k}}{L^3} \cosh k_2L, \quad M_4 = k_2^3 \cosh k_2L - \frac{\bar{k}}{L^3} \sinh k_2L;$$

$$P_1 = k_2^3 \sinh k_2L_1 - k_1^3 \sin k_1L_1, \quad P_2 = k_2^3 \cosh k_2L_1 + k_2k_1^2 \cos k_1L_1,$$

$$P_3 = -(k_2^3 \sinh k_2L_1 + N_1k_1^3 \sin k_1L_1 - N_3k_1^3 \cos k_1L_1),$$

$$P_4 = -(k_2^3 \cosh k_2L_1 - N_4k_1^3 \cos k_1L_1 + N_2k_1^3 \sin k_1L_1);$$

$$Q_1 = k_2^2 \cosh k_2L_1 + k_1^2 \cos k_1L_1, \quad Q_2 = k_2^2 \sinh k_2L_1 + k_2k_1 \sin k_1L_1,$$

$$Q_3 = -(k_2^2 \cosh k_2L_1 - N_1k_1^2 \cos k_1L_1 - N_3k_1^2 \sin k_1L_1),$$

$$Q_4 = -(k_2^2 \sinh k_2L_1 - N_4k_1^2 \sin k_1L_1 - N_2k_1^2 \cos k_1L_1);$$

$$R_1 = \frac{P_2Q_3 - P_3Q_2}{P_1Q_2 - P_2Q_1}, \quad R_2 = \frac{P_2Q_4 - P_4Q_2}{P_1Q_2 - P_2Q_1}, \quad R_3 = \frac{P_1Q_3 - P_3Q_1}{P_2Q_1 - P_1Q_2}, \quad R_4 = \frac{P_1Q_4 - P_4Q_1}{P_2Q_1 - P_1Q_2};$$

$$\Delta_1 = \cosh k_2L_1 + N_1 \cos k_1L_1 + N_3 \sin k_1L_1 - R_1(\cosh k_2L_1 - \cos k_1L_1) - R_3\left(\sinh k_2L_1 - \frac{k_2}{k_1} \sin k_1L_1\right),$$

$$\Delta_2 = \sinh k_2L_1 + N_4 \sin k_1L_1 + N_2 \cos k_1L_1 - R_2(\cosh k_2L_1 - \cos k_1L_1) - R_4\left(\sinh k_2L_1 - \frac{k_2}{k_1}\sin k_1L_1\right),$$

$$\Delta_3 = k_2 \sinh k_2L_1 - N_1k_1 \sin k_1L_1 + N_3k_1 \cos k_1L_1 - R_1(k_2 \sinh k_2L_1 + k_1 \sin k_1L_1) - R_3(k_2 \cosh k_2L_1 - k_2 \cos k_1L_1) - \Theta(k_2^2 \cosh k_2L_1 - N_1k_1^2 \cos k_1L_1 - N_3k_1^2 \sin k_1L_1),$$

$$\Delta_4 = k_2 \cosh k_2L_1 + N_4k_1 \cos k_1L_1 - N_2k_1 \sin k_1L_1 - R_2(k_2 \sinh k_2L_1 + k_1 \sin k_1L_1) - R_4(k_2 \cosh k_2L_1 - k_2 \cos k_1L_1) - \Theta(k_2^2 \sinh k_2L_1 - N_4k_1^2 \sin k_1L_1 - N_2k_1^2 \cos k_1L_1).$$

References

Anyfantis, N., Dimarogonas, 1983. Stability of columns with a single crack subjected to follower and vertical loads. International Journal of Solids and Structures 19, 281–291.

Atanackvic, T.M., Cveticanin, L., 1994. Dynamics of in-plane motion of a robot arm. In: Acar, M.J. Makra, Penny, E. (Eds.), Mechatronics. Computational Mech Publ, Boston, pp. 147–152.

Beck, 1952. Die Knicklast des einseitig eingespannten tangential gedruckten stabes. Zeitschrift für Angewandte Mathematik und Physik 3.

Bolotin, V.V., 1963. Non-Conservative Problems of the Theory of Elastic Stability. Macmillan, New York.

Carr, J., Malhardeen, M.Z.M., 1979. Beck's problem. SIAM Journal of Applied Mathematics 37, 261–262.

Cawley, P., Adams, R.D., 1979. A vibration technique for non-destructive testing of fibre composite structures. Journal of Composite Materials 13, 161–175.

Deineko, K.S., Leonov, M.IA., 1955. The dynamic method of investigating the stability of a bar in compression. PMM 19.

Dimarogonas, A.D., Paipetis, S.A., 1983. Rotor Dynamics. Elsevier, London.

Dzhanelidze, G. Iu., 1958. On the stability of a rod under the action of a follower force. Tr. Leningr. Politechn. In-ta. 192.

Feodos'ev, V.I., 1953. Selected problems and questions in strength of materials. Gostekhizdat.

Gounaris, G.D., Papadopoulos, C.A., 1997. Analytical and experimental crack identification of beam structures in air or in fluid. Computers and Structures 65, 633–639.

Gounaris, G.D., Papadopoulos, C.A., Dimarogonas, A.D., 1996. Crack identification in beams by coupled response measurements. Computers and Structures 58, 299–305.

Hanaoka, M., Washizu, K., 1979. Optimum design of Beck's column. Computers and Structures 11, 473–480.

Hauger, W., Vetter, K., 1976. Influence of an elastic foundation on the stability of a tangentially loaded column. Journal of Sound and Vibration 47, 296–299.

Jankovic, M.S., 1993. Comments on Eigenvalue sensitivity in the stability analysis of Beck's column with a concentrated mass at the free end. Journal of Sound and Vibration 167, 557–559.

Kikidis, M.L., Papadopoulos, C.A., 1992. Slenderness ratio effect on cracked beam. Journal of Sound and Vibration 155, 1–11.

Kounadis, A., 1983. The existence of regions of divergence instability for non-conservative systems under follower force. International Journal of Solids and Structures 19, 725–733.

Krawczuk, M., Ostachowicz, W.M., 1995. Modeling and vibration analysis of a cantilever composite beam with a transverse open crack. Journal of Sound and Vibration 183, 69–89.

Liebowitz, H., Vandervelt, H., Harris, D.W., 1967. Carrying capacity of a notched column. International Journal of Solids and Structures 3, 489–500.

Leipholz, H., 1983. Assessing stability of elastic systems by considering their small vibrations. Ingenieur- Archiv 53, 345–362.

Matsuda, H., Sakiyama, T., Morita, Ch., 1993. Variable cross sectional Beck's column subjected to non-conservative load. Zeitschrift fur angwandte Mathematik und Mechanik (ZAMM) 73, 383–385.

Nikolakopoulos, P.G., Katsareas, D.E., Papadopoulos, C.A., 1967. Crack Identification in Frame Structures. Computers and Structures 64, 389–406.

Papadopoulos, C.A., 1994. Torsional vibrations of rotors with transverse surface cracks. Computers and Structures 51, 713–718.

Pfluger, A., 1950. Stabilitats probleme der elastostatik. Springer-Verlag, Berlin.

Sundararajan, C., 1976. Influence of an elastic end support on the vibration and stability of Beck's column. International Journal of Mechanical Science 18, 239–241.

Sugiyama, Y., Katayama, K., Kinoi, S., 1995. Flutter of cantilevered column under rocket thrust. Journal of Aerospace Engineering 8, 9–15.

Timoshenko, S.P., Gere, J.M., 1961. Theory of Elastic Stability. McGraw-Hill International Book Company, Singapore.
Wang, Q., Quek, S.T., 2002. Enhancing flutter and buckling capacity of column by piezoelectric layers. International Journal of Solids and Structures 39, 4167–4180.
Wang, Q., Koh, C.G., 2003. On the region of flutter and buckling instability for a cracked beam. AIAA Journal 41, 2302–2304.